DOI: 10.1038/ncb2741

nature cell biology

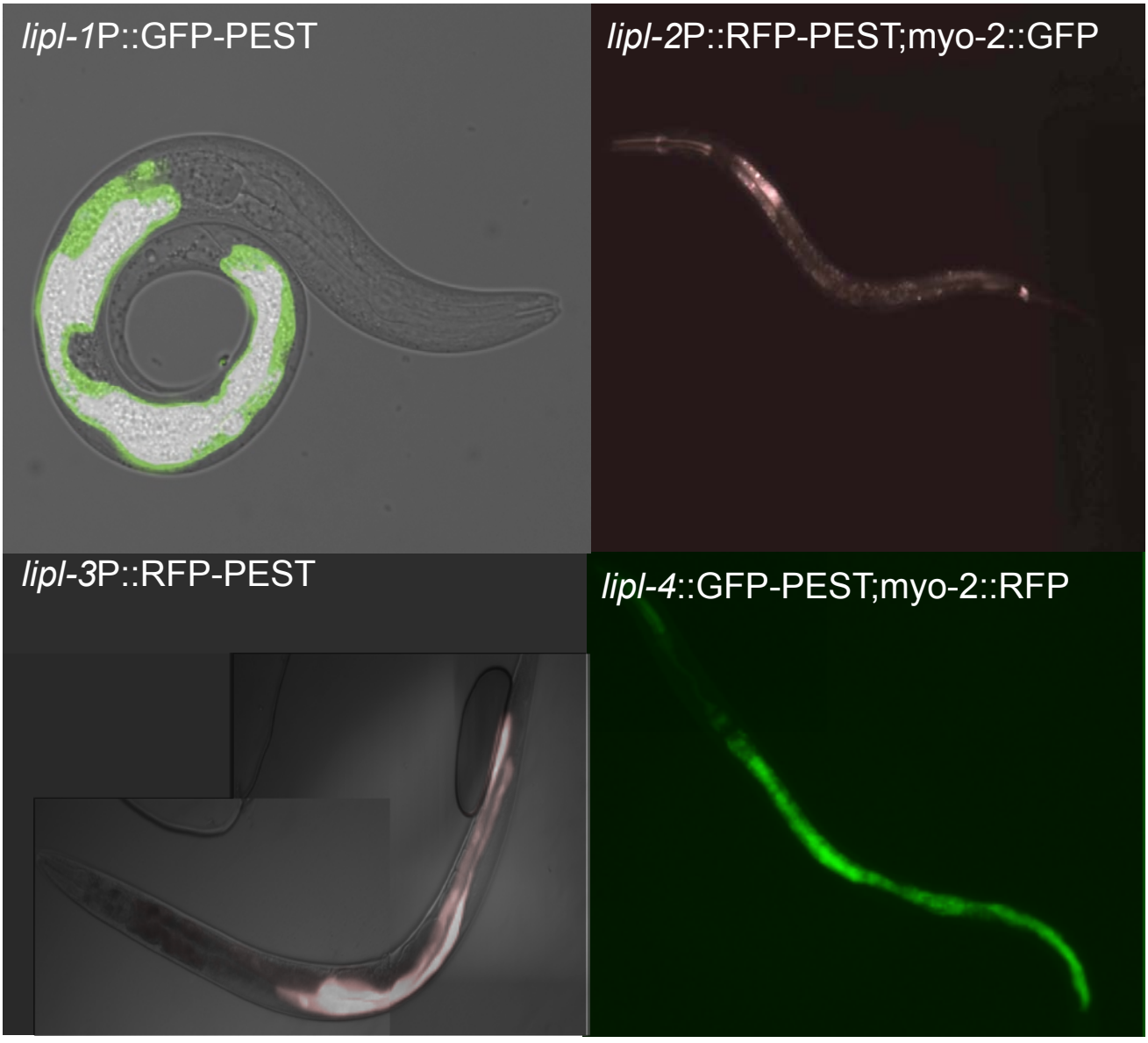

Figure S1 Fasting-responsive *lipl* genes are expressed in the *C. elegans* intestine. Wild-type animals carrying a transcriptional fusion of the *lipl-1* to *4* promoters to pest-carrying versions of GFP or mRFP were fasted in empty NGM plates. Patterns of expression after 16h of fasting are shown for *lipl-1* to *3* constructs. The pattern of expression of *lipl-4* in starvation-induced dauers is shown.

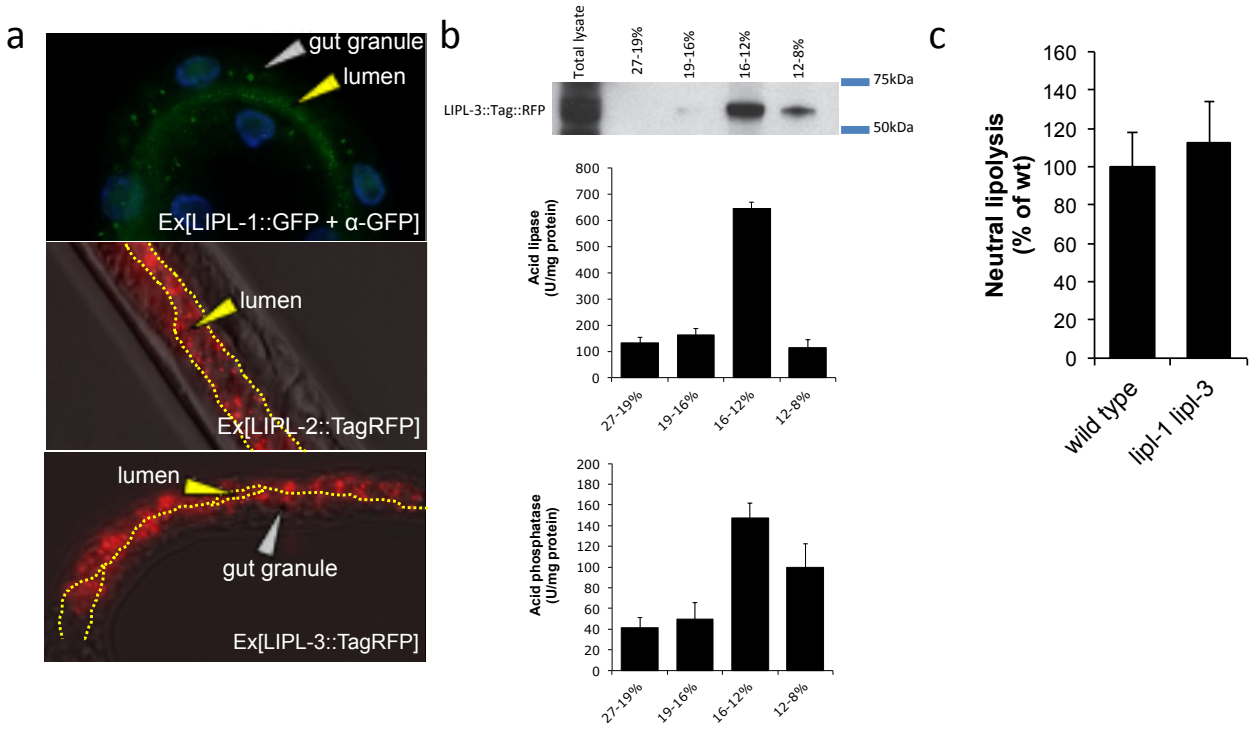

Figure S2 a. The LIPL proteins are expressed in the *C. elegans* acidic compartments. Immunostaining with anti-GFP (Roche) of LIPL-1::GFP, and patterns of expression of LIPL-2 and LIPL-3::TagRFP translational fusions are shown. In the LIPL-1 image, DAPI staining highlights the intestinal nuclei to help positioning LIPL-1. In LIPL-2 image, the picture was taken in the middle plane of the gut lumen, therefore the dotted lines marking the limits of the lumen are substantially separated and all the LIPL-2 comes from the lumen of the intestine. In LIPL-3 image, the picture is taken in a lateral plane of the gut lumen so that the luminal space is mostly not visible (only detectable were the yellow arrow points) and all the signal is observable in vesicles in the cytoplasm of the intestinal cells. The images fairly represent the actual location of the signal. **b,** LIPL-3 co-fractionates with the lysosomal compartment. Lysosomes were prepared from mixed stage *C. elegans*. *Top panel,* representative western blot of LIPL-3::TagRFP using anti-TagRFP antibody is shown (500 µg of protein were seeded per well). *Mid Panel,* Acid lipase activity per fraction (mean U/mg protein ±SEM), n=3 independent experiments. *Bottom Panel,* Acid phosphatase activity per fraction (mean U/mg protein ±SEM) (Biovision, USA), n=3 independent experiments. Fractions 16-8% were tested by western blot using antibodies that detect mitochondria (anti-HSP-60) or nuclei (anti-H3KMe19) and only background signal was detected in the lysosomal fraction. Total worm lysate was loaded as positive controls for different antibodies. Note that Tag::RFP and the acidic lipase activity co-fractionate with the canonical lysosomal acid phosphatase activity. **c.** *lipl-1 lipl-3* double mutant animals show normal neutral lipase activity. Neutral lipase activity was measured in 1-day adult whole lysates using QuantiChrom Lipase Assay, BioAssays Systems. Mean ±SEM are presented relative to wild type, n=3 independent experiments.

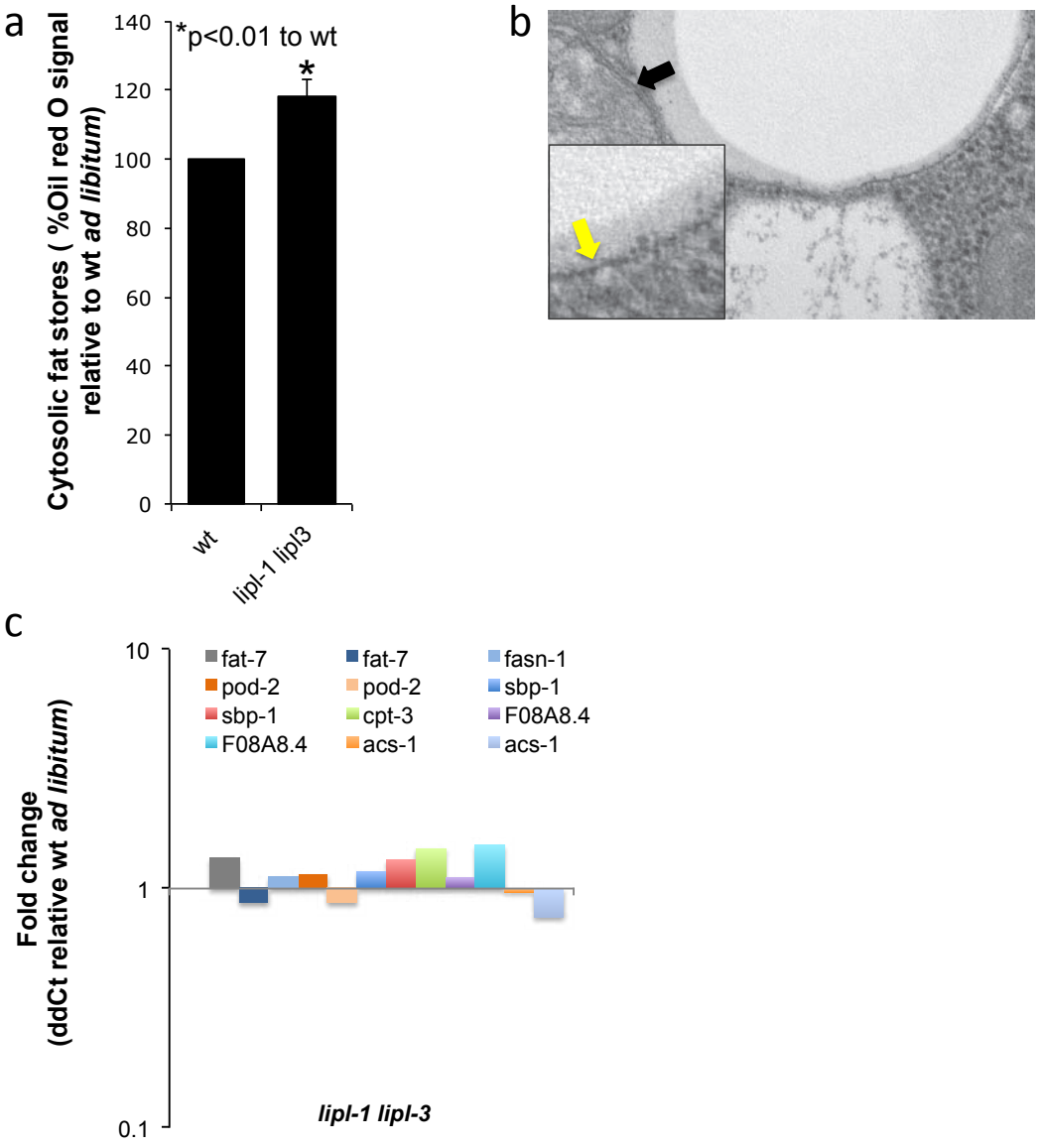

Figure S3 a, *lipl-1 lipl-3* animals have increased cytoplasmic fat levels. Oil red O signal in young-adult *lipl-1(tm1954) lipl-3(tm4498)* relative to wild-type worms is depicted as mean percentage ±%SEM, significant difference is marked, n=4 independent experiments. **b,** Lipid vesicles in TEM images are defined as empty or electron-light vesicles. Images show that the lipid monolayer vesicles (lipid vesicles) are the electron-light or empty cytosolic vesicles. The yellow arrow points to lipid monolayer and the black arrow points to an example of lipid bilayer. **c,** *lipl-1* and *lipl-3* loss of function does not alter β–oxidation or lipogenesis. The expression levels of *fat-7*, *fasn-1*, *pod-2* and *sbp-1* were used as readouts for the levels of lipogenesis as previously described (Van Gilst et al. 2005; Walker et al. 2010). The expression levels of *cpt-3*, *F08A8.4* and *acs-1* were used as a readout of β-oxidation as previously described (Van Gilst et al. 2005; Srinivasan et al. 2008). RNA was extracted from young fertile wild-type or *lipl-1 lipl-3* double mutant adults fed *ad libitum*. *dd*Cts were calculated normalizing to *ama-1* and the efficiency of the primer sets as previously described (Pfaffl 2001). Data from one representative experiment is presented (experiment was performed twice).

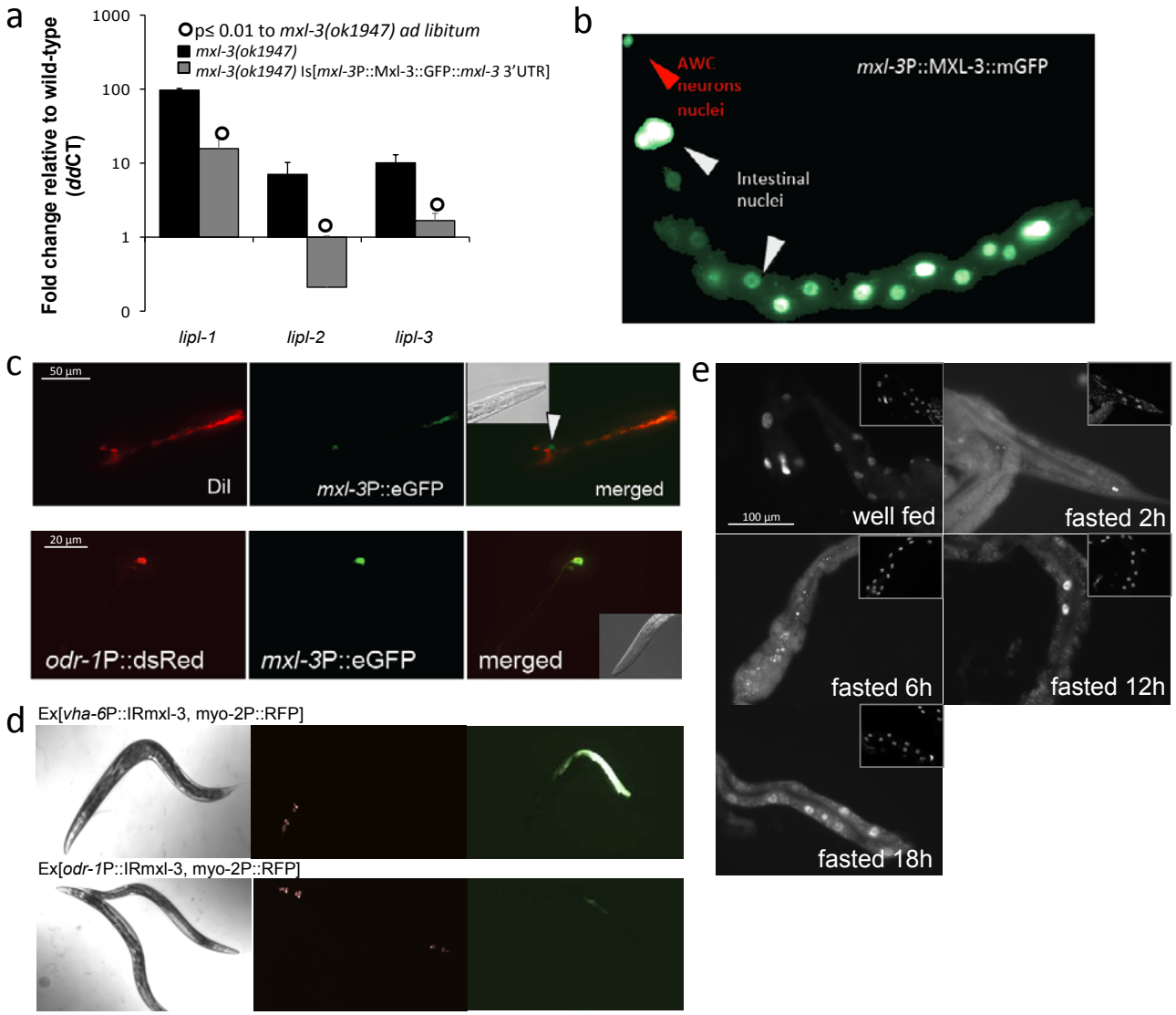

Figure S4. a, MXL-3::GFP construct is functional. The integrated MXL-3::GFP fusion with all endogenous regulatory elements shown in Fig. 1d was crossed into *mxl-3(ok1947)*. qRT-PCR analysis of mutant and transgenic animals, compared to wild-type worms, shows that this construct fully rescues *mxl-3(ok1947)* constitutive lipl upregulation. Mean *dd*CTs ±SEM are presented; all differences between *mxl-3(ok1947)* and the rescued strain are significant (p<0.001), n=3 independent experiments. **b,** MXL-3 localizes to nuclei of the intestine and a pair of sensory neurons. The pattern of expression of the rescuing translational fusion of MXL-3 to mGFP is shown. White arrowheads: intestinal nuclei, red arrowhead: sensory neuron nuclei. **c,** Neuronal MXL-3 signal corresponds to AWC sensory neurons. *Upper panels*, *mxl-3*P::eGFP-PEST animals were stained with DiI as previously described. *mxl-3*P::eGFP-PEST is expressed in a pair of sensory neurons that are not dye filled. *Lower panels*, Co-localization of Is[*mxl-3*P::eGFP-PEST] and Is[*odr-1::*dsRED]. *odr-1::*dsRED, generously provided by Cori Bargmann, is mostly expressed in AWC neurons. All together the data support MXL-3 is expressed in the nuclei of intestinal and AWC cells. **d**, Intestinal inactivation of *mxl-3* is sufficient to trigger a fasting-like transcriptional response. Inactivation through tissue-specific double stranded RNA expression of *mxl-3* is expected to reveal in which tissues MXL-3 is able to repress the lipl genes. *Upper panels*, Gut inactivation of *mxl-3* leads to transcriptional activation of *lipl-1*P::GFP. *Lower panels*, AWC inactivation has no effect on *lipl-1*P::GFP expression. **e,** MXL-3 transiently disappears from intestinal nuclei during fasting. Representative images or well-fed, 2, 6, 12 or 18h fasted young adults expressing low levels of MXL-3::GFP are presented. Worms were fixed, dissected, immunostained with aGFP antibodies, and also stained with DAPI (insets) to reveal nuclear localization and integrity. Images of well-fed condition were taken with 300ms exposure. Images of the fasted state were taken with 750ms exposure times. Quantification of MXL-3 positive nuclei relative to total intestinal nuclei (DAPI) is presented Fig. 3c.

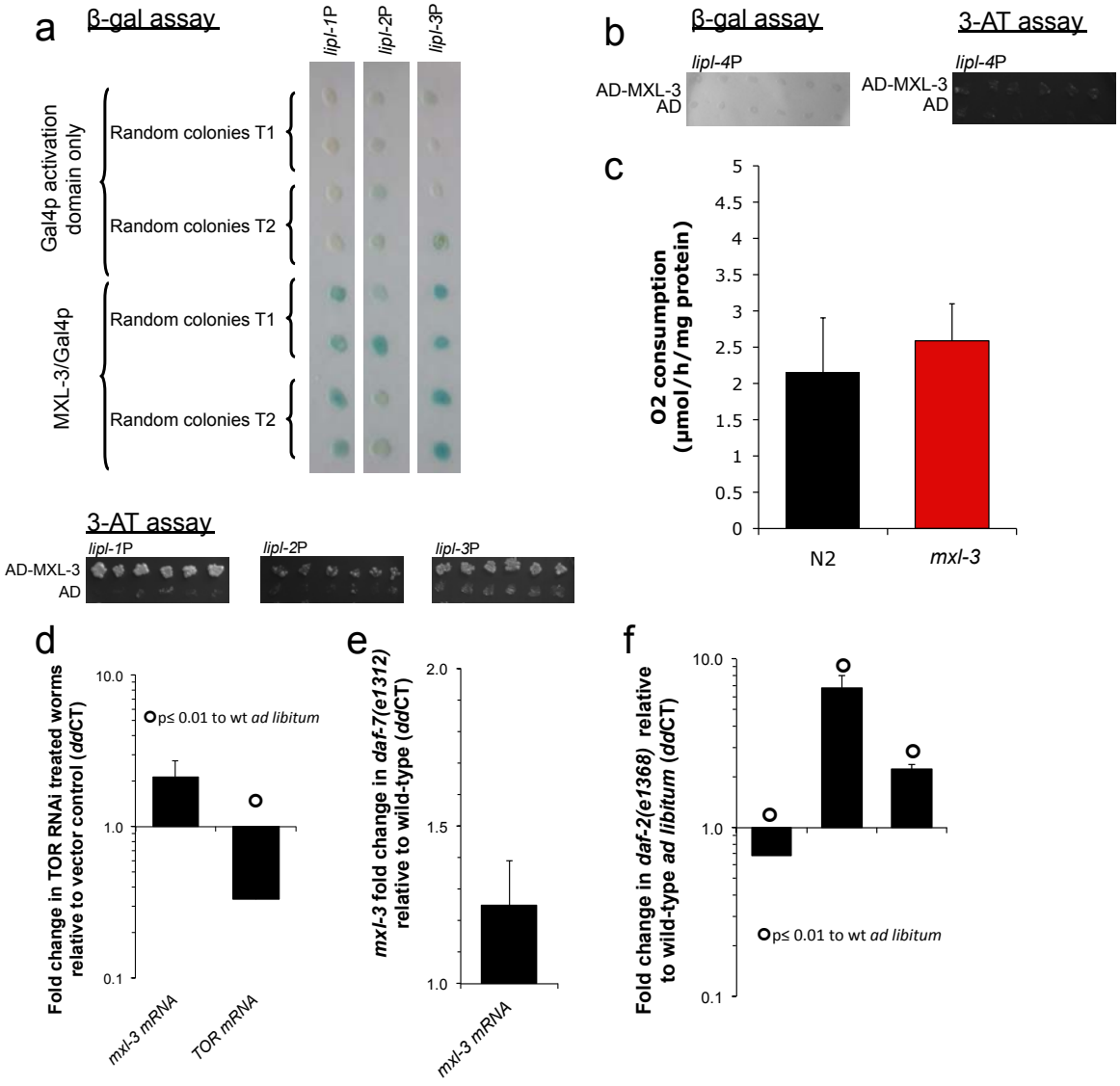

Figure S5 a, MXL-3 binds to the *lipl-1*, *lipl-2*, and *lipl-3* promoters. A subset of random colonies picked from transformations of yeast carrying *lipl-1* to *3* promoters after transformation with Gal-4 activation domain (AD) or AD fused to the MXL-3 ORF is shown. 97.9% and 95.8% of *lipl-1*, 54.1% and 79.2% of *lipl-2*, and 93.7% and 97.9% of *lipl-3*-promoter carrying colonies were activated by MXL-3 in ß–gal and 3-aminotriazole (3AT) assays, respectively, supporting that MXL-3 is able to bind and drive expression from the *lipl-1*, *lipl-2*, and *lipl-3* promoters. **b,** MXL-3 does not bind to the *lipl-4* promoter. As representative random transformants show, only control levels of colonies (less than 5%) gave any ß–gal signal or grew on 3AT when *lipl-4* promoter carrying yeast clones were transformed with AD-MXL-3, supporting that MXL-3 does not bind to the *lipl-4* promoter. **c,** *mxl-3(ok1947)* animals show wild-type oxygen consumption. O_2 consumption was measured as previously described (Soukas et al. 2009). Median ± St Dev of the µmoles of O_2 consumed per hour per mg of worm is depicted. **d,** CeTOR inhibition does not repress *mxl-3* transcription. Animals treated from late L3 stage with RNAi against TOR or vector control were harvested as young adults. Mean +SEM of 3 independent experiments are depicted. **e,** TGF-β inhibition does not repress *mxl-3* transcription. Wild-type or *daf-7(e1312)* animals raised from late L3 at 25°C were harvested as young adults. Mean +SEM of 3 independent experiments are depicted. **f,** Impaired insulin signaling is insufficient to fully repress *mxl-3* transcription. Wild-type or *daf-2(e1368)* animals raised from late L3 at 25°C were harvested as young adults. RNA was extracted and analyzed as described below. *ddCts* were calculated normalizing to *ama-1* and the efficiency of the primer sets as previously described (Pfaffl 2001). Mean +SEM of 3 independent experiments are depicted, significant differences are indicated.

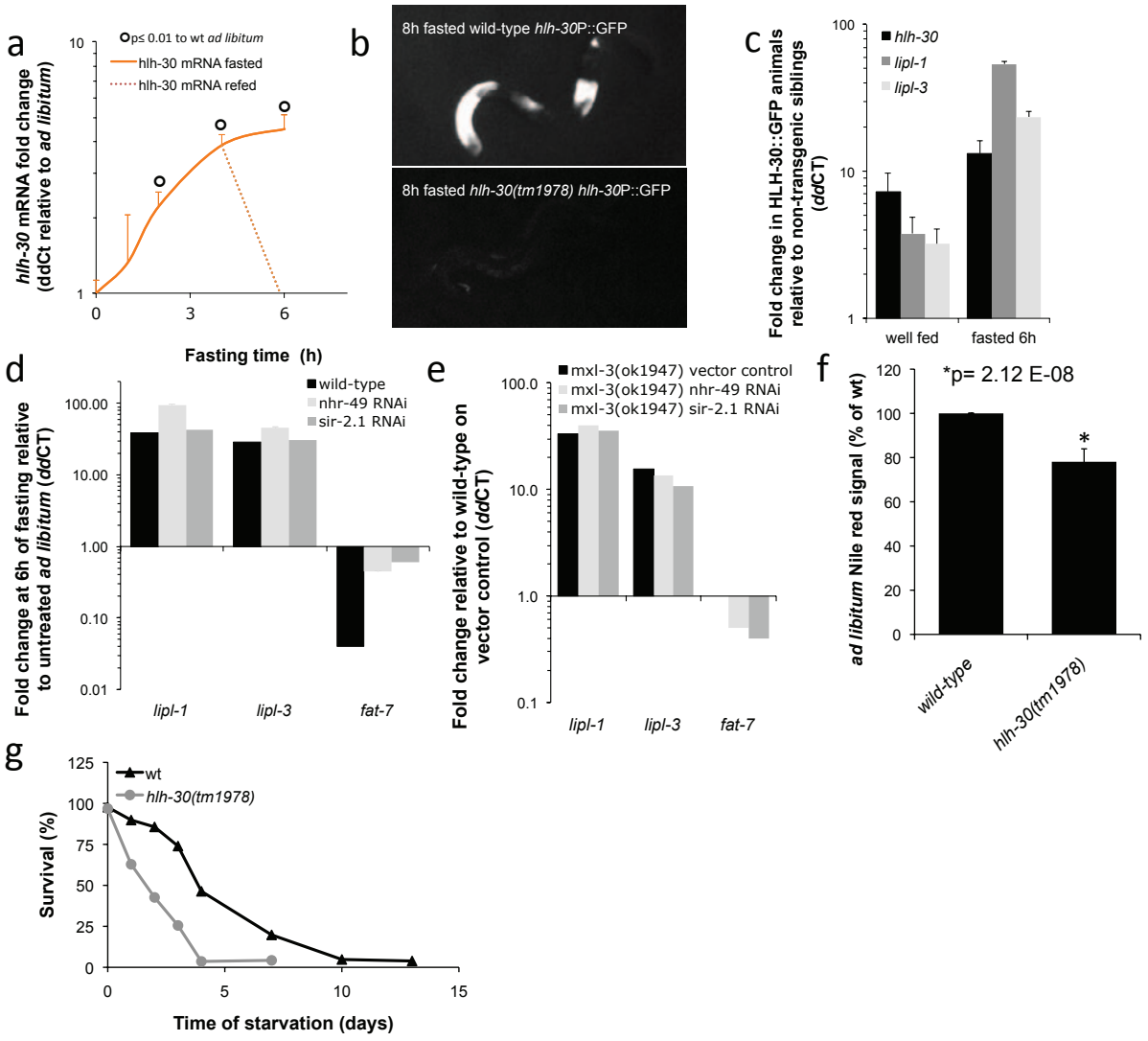

Figure S6 a, *hlh-30* is transcriptionally regulated according to food availability. Young adults were fasted or fed *ad libitum* and samples were collected at the indicated time periods. A subpopulation of the fasted worms was re-fed after 4h of food deprivation and harvested 2 h later. ∂∂Cts were calculated as in Fig.1. Mean + SEM are depicted. Significant statistical differences as compared to *ad libitum* at the same time points are indicated (º), n=3 independent experiments. **b,** HLH-30 controls its own transcription. 8h fasted wild-type or *hlh-30(tm1978)* mutant L3 animals expressing an *hlh-30* transcriptional reporter (*hlh-30*P::GFP) are depicted. **c,** High *hlh-30* transcriptional levels are insufficient to fully activate lysosomal lipolysis. Expression levels of *hlh-30*, *lipl-1*, and *lipl-3* were measured in HLH-30::GFP transgenic animals and non-transgenic siblings well-fed or fasted for 6h. *ddCts* were calculated as in Fig.1. Mean + SD of 3 independent experiments are depicted. Differences to wild-type *ad libitum* are all significant (p<0.01). Differences between HLH-30::GFP *ad libitum* and fasted are significant for *lipl-1* and *lipl3* (p<0.01)**. d,** NHR-49/CePPRα or SIR-2.1 are not required to activate *lipl-1* **or** *lipl-3* upon fasting. Expression levels of *lipl-1* and *lipl-3* were measured in well-fed and 6h fasted *nhr-49* and *sir-2.1* RNAi treated animals. *ddCts* were calculated as in Fig.1. Representative experiment is depicted. Experiment was performed twice. *fat-7* expression is a positive control. **e,** NHR-49/CePPRα or SIR-2.1 do suppress the *mxl-3* constitutive induction of the *lipl-1* **or** *lipl-3* genes. Expression levels of *lipl-1* and *lipl-3* in *mxl-3(ok1947)* reared on vector control or RNAi against *nhr-49* or *sir-2.1* were measured. *ddCts* were calculated were calculated as described above. Representative experiment is depicted. Experiment was performed twice. *fat-7* expression is a positive control. **f,** *Ad libitum*-fed HLH-30-deficient animals show reduced LRO content. Live Nile red signal in well-fed young-adult *hlh-30(tm1978)* animals. Mean ± SEM relative to well-fed wild-type worms is depicted, significant difference is marked, n=3 independent experiments. **g,** *hlh-30* is required for optimal survival to starvation. Representative starvation survival curve of L4 larvae was measured as described in Supporting Online Material.

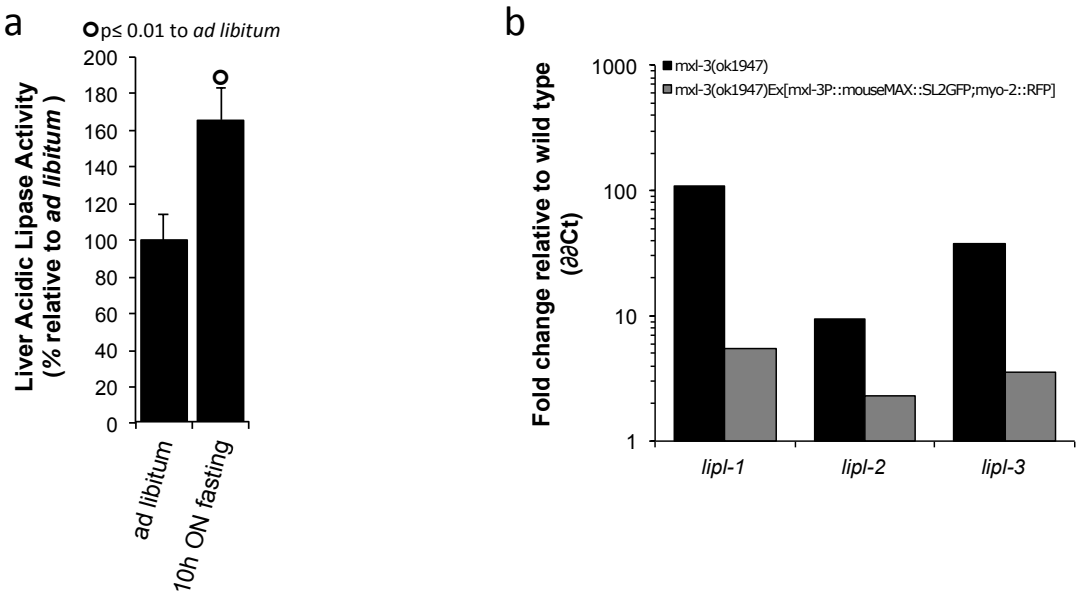

Figure S7 a, Lysosomal lipase activity is more abundant in the liver of fasted mice**.** Acidic lipase activity in the liver of C57BL/6J 9-week females fasted overnight for 10h relative to siblings feeding *ad libitum* is shown as % ±%SEM, n=3 independent experiments. **b,** Mouse MAX rescues the constitutive activation of *lipl-1* and *lipl-3* observed in *mxl-3* mutant worms. Mouse MAX was cloned from mouse white cells cDNA into a polycistronic SL2 construct and injected in *mxl-3(ok1947)* mutant animals. qRT-PCR analysis of mutant transgenic animals and mutant non-transgenic siblings compared to wild-type worms shows that this construct rescues *mxl-3(ok1947) lipl* induction. *ddCts* were calculated normalizing to *ama-1* and the efficiency of the primer sets as previously described (Pfaffl 2001). . Representative experiment is depicted. Experiment was performed with two independent lines.

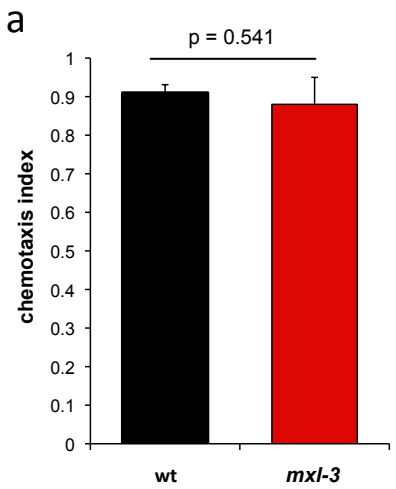

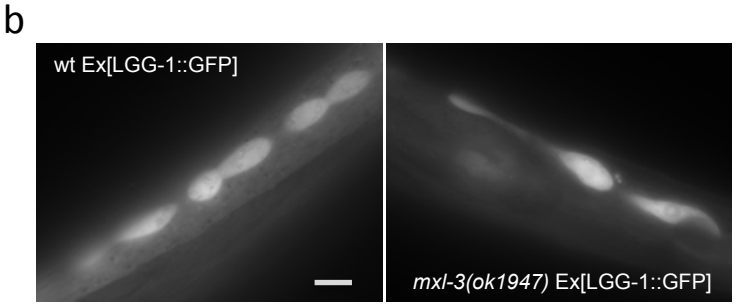

	Autophagic punctae/cell (n=50)	
	Mean	Significance
wild type Ex[LGG1::GFP])	1.751	
mxl-3(ok1947 Ex[LGG1::GFP])	1.946	0.233

Figure S8. a, *mxl-3* animals have wild-type chemosensory abilities. Five populations of ~100 wild-type or *mxl-3(ok1947)* worms were scored for their chemotaxis towards a 1:100 point source of isoamyl-alcohol as previously described. Median ±SEM of the chemotaxis indexes is depicted (n= 5 independent experiments). Statistical analysis was carried out using pairwise student's t-test. **b,** *mxl-3* animals do not show increased autophagy. Representative images of seam cells of well-fed wild-type and *mxl-3(ok1947)* animals carrying LGG-1::GFP imaged in an Axioplan microscope (Zeiss). The table shows the quantification of GFP::LGG-1 punctae per cell, n=3 independent experiments.

Supplementary Table Legends

Supplementary Table 1. Nutrition-responsive candidate genes.
Genes were selected for qRT-PCR analysis of transcriptional levels upon fasting if they were present in at least 2 of the following lists of genes: starved *C. elegans* larval stage 1 (L1) (*1*), glucose deprived *Drosophila melanogaster* (*2*), mouse liver upon fasting (*3*), genes differentially expressed at the dauer stage (*1*), and genes that when inactivated lead to increased or decreased Nile red levels (*4*). Some genes were tested because of particularly interesting annotations or known/predicted functions or other previous reports.

Supplementary Table 2. Available functional descriptions of the genes tested to transcriptionally respond to fasting (source Wormbase).

Supplementary Table 3. Transcriptional regulators screened for a role in *lipl-1* **expression.**
Genes were selected by searching for the term transcriptional regulator and/or nuclear hormone receptor. Screening clones were pooled from Ahringer, Vidal, or both RNAi libraries when available. Ahringer-based transcription factor library was built and generously provided by Sean Curran and David Simon. Nuclear-hormone receptor library was generated and generously provided by Ho Yi Mak.

Supplementary Table 4. HLH-30-dependent autophagic genes.
Genes which upregulation in fasted worms was observed to be HLH-30 dependent because they were not upregulated in fasted *hlh-30(tm1978*) fasted animals are listed. Young adult wild-type or *hlh-30(tm1978)* worms were fasted for 8h at 20C, frozen in liquid nitrogen and later processed for RNA extraction as described in Supplementary Materials and Methods. Levels of expression relative to well-fed wild-type animals are presented as mean ddCT ± SEM of 3 independent experiments.

Supplementary Table 5. MXL-3 controls lifespan from the *C. elegans* **intestine.** Intestinal expression of *mxl-3* rescues the extended lifespan phenotype of mxl-3(ok1947). Data are presented as mean lifespan (LS) ± standard error of the mean (SEM). Kaplan-Meier statistics calculated using SSPS17 statistics package are shown. Symbols: **a.** number of uncensored animals is depicted (animals that crawled off the plate, bagged, exploded, or became contaminated were censored); **b.** OP50 bacteria; **c.** compared to *mxl-3(ok1947)*; **3**. 22°C.

Supplementary Table 6. *mxl-3* **longevity phenotype is additive to canonical genetic models of longevity.** Epistasis analyses of *mxl-3* extended lifespan phenotype are presented as mean lifespan (LS) ± standard error of the mean (SEM). Kaplan-Meier statistics calculated using SSPS17 statistics package are shown. Symbols: **a.** number of uncensored animals is depicted (animals that crawled off the plate, bagged, exploded, or became contaminated were censored). Symbols: **a.** number of uncensored animals is depicted (animals that crawled off the plate, bagged, exploded, or became contaminated were censored); **b.** OP50 bacteria; **c.** compared to *mxl-3(ok1947)* or *mxl-3* RNAi; **e.** compared to *skn-1(zu67)*; **f.** compared to *daf-16(mu86)*; **1.** 20°C; **2.** 25°C; **3**. 22°C

Supplementary Table 7. *mxl-3* **longevity phenotype is additive to caloric-restriction and food removal.** Epistasis analyses of *mxl-3* extended lifespan phenotype are presented as mean lifespan (LS) ± standard error of the mean (SEM). Kaplan-Meier statistics calculated using SSPS17 statistics package are shown. Symbols: **a.** number of uncensored animals is depicted (animals that crawled off the plate, bagged, exploded, or became contaminated were censored). Symbols: **a.** number of uncensored animals is depicted (animals that crawled off the plate, bagged, exploded, or became contaminated were censored); **b.** OP50 bacteria; **c.** compared to *mxl-3(ok1947)* or *mxl-3* RNAi; **d.** compared to wt on *pha-4* RNAi; **g.** compared to wt on *rheb-1* RNAi; **h.** compared to wt on *bec-1* RNAi; **1.** 20°C; **3**. 22°C.

Supplementary Table 8. *mxl-3* **longevity phenotype is independent from autophagy.** Epistasis analyses of *mxl-3* extended lifespan phenotype are presented as mean lifespan (LS) ± standard error of the mean (SEM). Kaplan-Meier statistics calculated using SSPS17 statistics package are shown. Symbols: **a.** number of uncensored animals is depicted (animals that crawled off the plate, bagged, exploded, or became contaminated were censored). Symbols: **a.** number of uncensored animals is depicted (animals that crawled off the plate, bagged, exploded, or became contaminated were censored); **d.** compared to wt on *pha-4* RNAi; **h.** compared to wt on *bec-1* or *atg-16.2* RNAi; **1.** 20°C; **3**. 22°C.